Chapter 3

# Molecular Interactions

## Contents

## 3.1 Introduction

When molecules are near each other, they can influence one another. Therefore, the balance between the forces of attraction and repulsion needs to be understood. Such forces must exist in reality otherwise there would be nothing to bring molecules together to form liquid and solid states. People have speculated about these intermolecular forces since the concept of atoms and molecules first existed. The present theory is that molecules attract at long range but repel strongly at short range.

## 3.2 Molecular Force Fields

Actual interactions between atoms is in the realm of physical chemistry. For computational simulations, these interactions are too complex to simulate systems larger than a couple of molecules on the current computers available. Therefore, it is common practise to represent these real interactions as a computational force field. The choice of computational method is dependent on the size of the system and the time scales of calculations. For systems with up to several hundred to several thousand atoms, the molecules can be represented as individual atoms with each atom represented by a sphere. There are many types of force field, but they all follow a similar pattern:

- Nuclei and electrons are combined in an atom, represented by a ball.
- A ball has a radius and a constant charge. The ball can vary in softness.
- Bonds are represented by springs.
- Springs have an equilibrium length and can vary in stiffness.

The interactions between these spheres form the molecular force field. The interactions are described by pre-assigned parameters, that are system dependent. These parameters can be obtained from experiment and/or higher level computational calculations, such as *ab-initio*. The force field is the set of parameters used in classical mechanical calculations. The potential energy of the system is described by the sum of all the interactions within the system, equation 3.2.1, where $E_{str}$ is the energy function for stretching a bond between two atoms, $E_{bend}$ is the energy required for bending an angle between three atoms, $E_{tors}$ is the torsional energy for rotation around a bond, $E_{VdW}$ is the Van der Waals energy, $E_{el}$ is the electrostatic energy, and $E_{Xterms}$ represents any coupling between the above terms.

$$E_{FF} = E_{str} + E_{bend} + E_{tors} + E_{VdW} + E_{el} + E_{Xterms} \tag{3.2.1}$$

The first three terms represent the bonded interactions. The electrostatic and Van der Waals energies are non bonded interactions between atoms. To be able to calculate the force field energy it is necessary to know atomic coordinates, geometries, and the relative energies of the atoms in the system.

The calculation of the total potential energy is dominated by the number of non-bonded interactions. The time for calculation of the bonded interactions increase on the order of $\sim N$, while the time for calculation of the non-bonded interactions increase on the order of $\sim N^2$.

### 3.2.1 Stretching energy

The stretching energy of a bond is the energy of the extension of the spring, bonding two atoms, Figure 3.1. The shape of the energy curve is well described by a Taylor expansion, equation 3.2.2, where $r_0$ is an equilibrium bond length for the given system and so corresponds to the minimal energy.

$$E_{str}\left(r^{AB}-r_0^{AB}\right)=E\left(r_0\right)+\frac{\mathrm{d}\,E}{\mathrm{d}\,r}\left(r^{AB}-r_0^{AB}\right) + \frac{1}{2}\frac{\mathrm{d}^2\,E}{\mathrm{d}\,r^2}\left(r^{AB}-r_0^{AB}\right)^2+\frac{1}{6}\frac{\mathrm{d}^3\,E}{\mathrm{d}\,r^3}\left(r^{AB}-r_0^{AB}\right)^3+\mathcal{O}\left(r^4\right) \quad (3.2.2)$$

At $r = r_0$, $E(r_0)$ is zero and is used as the zero point on the energy scale, the second term is a first order derivative that is also close to zero. The cubic term will drive the energy of the bond to negative value at infinity, so the formulation is often simplified to an harmonic interaction, equation 3.2.3, where $k^{AB}$ is the force constant for stretching the bond between atoms A and B and will change depending on the system.

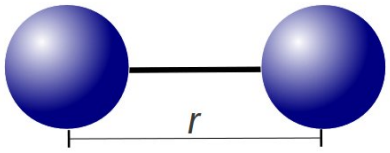


Figure 3.1: Model of diatomic molecule with bond length $r_0$.

$$E_{str}=\frac{1}{2}k^{AB}\left(r^{AB}-r_0^{AB}\right)^2 \quad (3.2.3)$$

Approximation to harmonic form is sufficient for most molecular dynamics calculations. For calculations of bond length dependent parameters, such as vibrational frequencies, or when the starting configuration is much different from equilibrium, terms up to the forth order may be included. The other common choice is the Morse potential [1], equation 3.2.4, where $\alpha=\sqrt{k/2D^{AB}}$ and $D^{AB}$ is the bond dissociation energy, i.e. the depth of the well.

$$E_{str}=D^{AB}\left(1-\exp\left(-\alpha\left(r^{AB}-r_0^{AB}\right)^2\right)\right) \quad (3.2.4)$$

The Morse potential reproduces stretching well over a wide range of distances, at long distances tends to zero. Hence the Morse potential is slow in bringing atoms to equilibrium bond lengths, when the initial geometry has a large bond length. The comparison between harmonic and Morse potentials is shown in Figure 3.2.

The stretching energy has the highest contribution to overall energy of the system, followed by the bending energy.

### 3.2.2 Bending Energy

Similarly to the stretching energy, bending energy can also be expressed by a Taylor expansion, that can then be approximated to a harmonic potential, equation 3.2.5, where $\theta^{ABC}$ is an angle between three atoms *A, B* and *C*, as shown in Figure 3.3, and $k^{ABC}$ is the force constant for the bending between three given atoms.

$$E_{bend}=\frac{1}{2}k^{ABC}\left(\theta^{ABC}-\theta_0^{ABC}\right)^2 \quad (3.2.5)$$

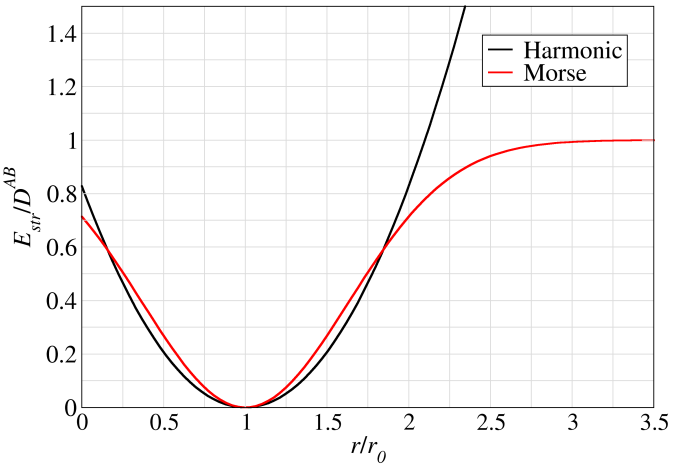


Figure 3.2: Bond stretching energy. Harmonic potential compared to the Morse potential.

When a higher accuracy is required for the calculation, the next highest order term in the expansion can be included, or a series of harmonic potentials can be used.

Changes in the bending energy are usually smaller than the changes in stretching energy, so less energy is required to distort bond angles in comparison to bond length. Hence, force constants for bending are proportionally smaller than those for stretching.

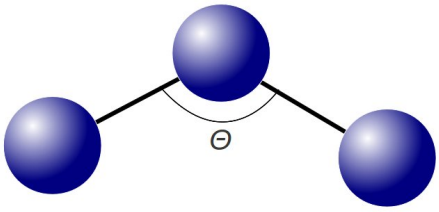


Figure 3.3: An angle between three bonded atoms.

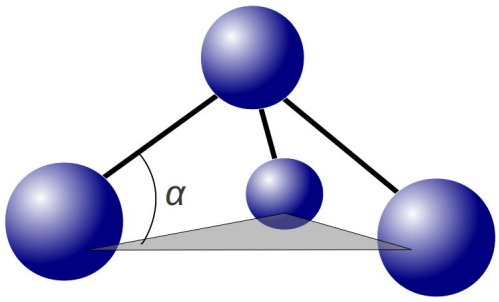


Figure 3.4: An illustration of out-of-plane bending, created by three atoms bonded to $sp2$ hybridised central atom.

When the central atom $B$ is bonded to more than two other atoms, as shown on the Figure 3.4, a pyramidal structure is formed. This angle can no longer be calculated in the manner discussed above. A high force constant should be used to penalise out-of-plane bending, this will make planar structures very inflexible. By introducing a new term, the flexibility of the planar structure is maintained while out-of-plane movement is also taken into account. This bending is often referred to as the improper torsional energy. This also often takes the form of a harmonic potential, equation 3.2.6.

$$E_{improper} = \frac{1}{2}k^B(\alpha)^2 \tag{3.2.6}$$

### 3.2.3 Torsional Energy

Four aligned atoms frequently will rotate along the central bond, as shown in Figure 3.5.

Rotation along the bond is continuous, so when the bond rotates by $360°$ the energy should return to the initial value, making torsional energy periodic. The potential is well

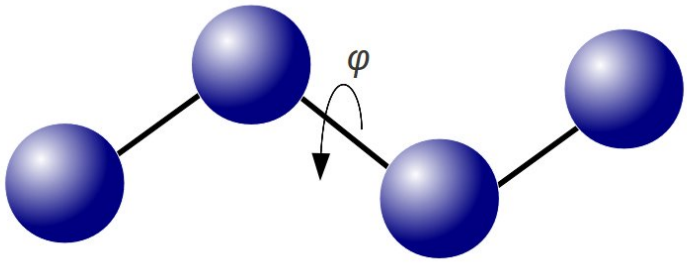


Figure 3.5: Torsional / dihedral angle, created by four linearly aligned atoms.

represented by the Fourier series, equation 3.2.7, where $n$ is a periodicity term, depending on the allowed rotation it can be $n = 1$ for full $360°$ rotation, $n = 2$ for $180°$ periodicity, $n = 3$ for $120°$ periodicity, etc. $V_n$ is a constant determining the barrier for the rotation, $V_n$ is not equal to zero for allowed periodic rotations, $\varphi$ is the torsional angle (also called the dihedral angle) and is shown on the Figure 3.5.

$$E_{tors} = \sum_n V_n \cos\left(n\varphi - \varphi_0\right) \tag{3.2.7}$$

Figure 3.6 shows a plot of the two torsional potentials with $n = 3$, $V_n = 4$ (dashed line), $n = 2$, $V_n = 3$ (solid line) and the corresponding total torsional potential in red if the two are combined.

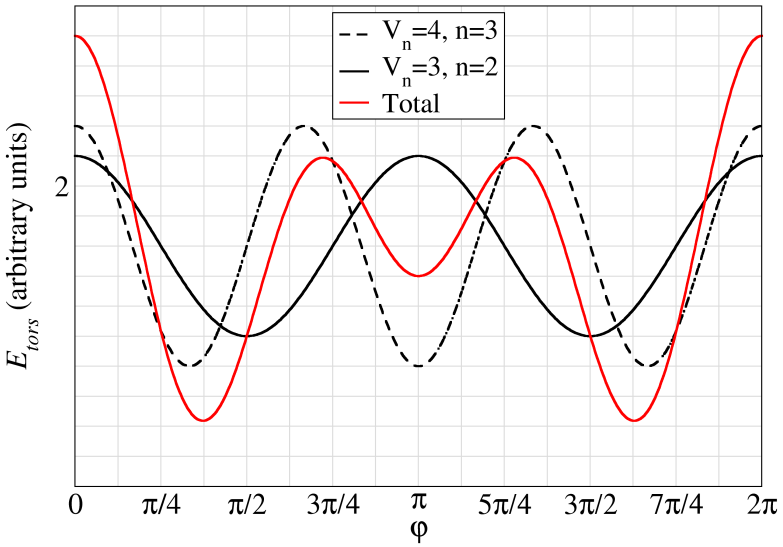


Figure 3.6: Variation of torsional potential for different values of $n$ and $V_n$ and the total potential (red).

### 3.2.4 Van der Waals

In addition to the bonded interactions described above, there are non bonded interactions in the system. These interactions appear between atoms in the same or neighbouring molecule and are normally described by two potentials, representing the Van der Waals energy and the electrostatic energy.

The Van der Waals energy describes the repulsion and attraction between non bonded atoms. At large interatomic distances the Van der Waals energy goes to zero, whereas at short distances it is positive and very repulsive. This mimics the overlap of the negatively charged electronic clouds of atoms. At intermediate distances there is a mild attraction between electronic clouds, due to electron-electron correlation. The attraction between two atoms arises because of an induced dipole–dipole moment created by the motion of electrons through the molecule, which effects the neighbouring molecule. The attraction between two fragments does not only depend on dipole–dipole interactions, but also on dipole–quadrupole, quadrupole–quadrupole etc. interactions. These interactions do not have a high contribution to the overall energy, so for simplicity they are neglected in calculations.

In 1903, Gustav Mie proposed an intermolecular pair potential [2], comprising two parts to represent attractive and repulsive forces, equation 3.2.8, where $r$ is interatomic distance, $\epsilon$ is the depth of the well at $\sigma$, the interatomic separation at which repulsive and attractive terms balance out and $m, n$ can be adjusted.

$$E_{pair}(r) = \left(\frac{n}{n-m}\right)\left(\frac{n}{m}\right)^{m/(n-m)} \epsilon \left[\left(\frac{\sigma}{r}\right)^{n} - \left(\frac{\sigma}{r}\right)^{m}\right] \tag{3.2.8}$$

There have been a number of models suggested, where $m$ and $n$ take different values and show an accurate representation of experimentally known interactions [3, 4]. Nevertheless, the most popular one is the 12–6 Lennard-Jones potential [5], equation 3.2.9, where $\sigma$ is the interatomic separation at which repulsive and attractive terms balance out and $\epsilon$ is the depth of the well. The usage of 12 term reduces the amount of calculations needed, making it the lightest method available.

$$E_{VdW}^{LJ} = 4\epsilon^{AB}\left[\left(\frac{\sigma^{AB}}{r^{AB}}\right)^{12} - \left(\frac{\sigma^{AB}}{r^{AB}}\right)^{6}\right] \tag{3.2.9}$$

The 12–6 Lennard-Jones potential is shown on the Figure 3.7. Red shows the repulsive term, blue the attractive term and the overall potential is shown in black. Position of $\sigma$ and $\epsilon$ is also shown on the graph.

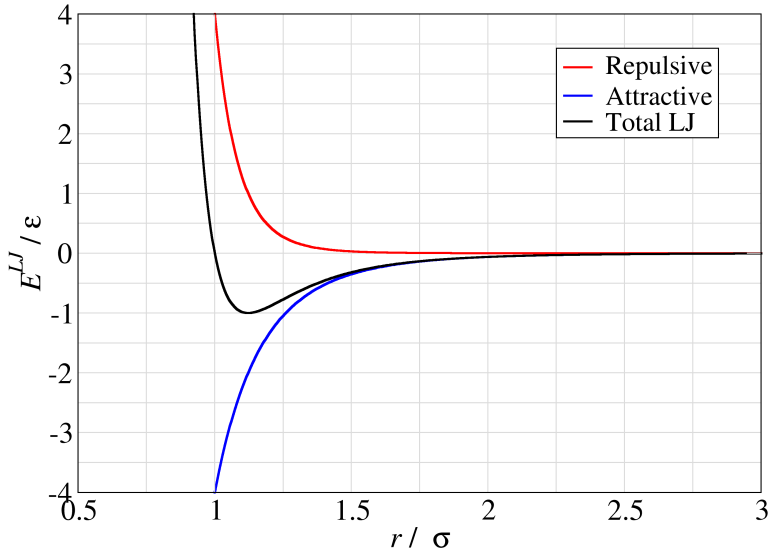


Figure 3.7: The Lennard-Jones Potential (black) is a combination of attractive (blue) and repulsive (red) terms.

It is possible to mix two Lennard-Jones potentials for single type atoms to obtain a potential describing interaction between two different atoms. There are three main approaches:

- Arithmetic or Lorentz-Berthelot rules, equations 3.2.10 and 3.2.11 [6].

$$\sigma_{ij} = \frac{\sigma_{ii} + \sigma_{jj}}{2} \tag{3.2.10}$$

$$\epsilon_{ij} = \sqrt{\epsilon_{ii}\epsilon_{jj}} \tag{3.2.11}$$

- Geometric rules equation 3.2.12, with $\epsilon_{ij}$ calculated as given in equation 3.2.11 [7].

$$\sigma_{ij} = \sqrt{\sigma_{ii}\sigma_{jj}} \tag{3.2.12}$$

- Fender-Halsey rule, equation 3.2.13 [8].

$$\epsilon_{ij} = \frac{2\epsilon_i\epsilon_j}{\epsilon_i + \epsilon_j} \tag{3.2.13}$$

A slightly more accurate potential, but up to 4 times more computationally demanding, is the Buckingham or Hill potential [4]. Repulsive forces take the form of an exponential, as the repulsion arises due to electron correlation, and the electron density reduces exponentially with the distance, equation 3.2.14, where $A, B$, and $C$ are suitable constants.

$$E_{VdW}^{Hill} = A\exp\left(-Br_{AB}\right) - Cr_{AB}^{6} \tag{3.2.14}$$

### 3.2.5 Electrostatic Energy

The electrostatic energy calculates non bonded interactions that appear due to an uneven internal distribution of electrons. This leads to positively and negatively charged parts in molecule. The simplest way to model this behaviour is to place charges on atoms. The law of the interaction between two point charges was investigated by Charles Augustin Coulomb in 1780s and can be expressed by the Coulomb potential, equation 3.2.15, where $\epsilon_0$ is the dielectric constant, the $Q$ values are partial electronic charges on atoms A and B, and $r$ is a distance between them.

$$E_{el} = \frac{1}{4\pi\epsilon_0}\frac{Q^A Q^B}{r^{AB}} \tag{3.2.15}$$

The atomic charges are mainly taken from electrostatic potential calculations carried out using higher precision methods. Another approach arises from assigning bond dipole moments. This gives similar results to the partial charge method, but these two methods will only give identical results for interactions at larger distances.

### 3.2.6 Cross Terms

There are also cross terms available for some force fields. These can cover the coupling between the fundamental stretching, bending and torsional interactions.

## 3.3 Choice of Force Field

The correct choice of the force field is essential for performing an accurate simulation. A large number of force fields have been developed through last decades. The force field consists of a set of parameters that depend on a particular the atom and the interaction.

Ideally force fields are designed to be transferable between a number of molecular systems. Nevertheless, some are more suitable for particular systems and states, then others. Comparison of the performance of the force filed should be done with a specific study in mind. Typical tests include the comparison to the experimental physical properties, such as density, boiling and melting temperatures, secondary protein structure, as well as the agreement with vapour-liquid coexistence, and the reproduction of thermodynamic properties.

Most force fields represent all atom systems, with a few being united atom where hydrogens are united to the neighbouring heavy atoms. United atom representation has less interactions, by such speeding up the calculations. Not every system can be accurately represented as united atom, for example systems having hydrogen bonding, benzene rings, polar and charged systems.

All atom force fields:

- OPLS-AA(Optimised Potentials for Liquid Simulations) [9]
- CHARMM (Chemistry at HARvard Macromolecular Mechanics) [10]
- AMBER (Assisted Model Building with Energy Refinement) [11]
- UFF (Universal Force Field) [12]

United atom force fields:

- OPLS (Optimised Potentials for Liquid Simulations)[13]
- CHARMM (Chemistry at HARvard Macromolecular Mechanics) [10]
- GROMOS (GROningen MOlecular Simulation) [14]
- TraPPE (Transferable Potentials for Phase Equilibria) [15]

### 3.3.1 Universal Force Field (UFF)

UFF [12] was developed by Rappe *et. al.* in 1992. It is an unusual force field, unlike others it covers the full periodic table, from hydrogen to lawrencium. The parameters are obtained by estimating from given general rules, that convert individual parameters for the element into the intermolecular and intramolecular parameters for calculations.

The performance of this force field with respect to the experimental results [16], is not very consistency, so it is not really suitable for high accuracy condensed state calculations. This force field is however useful for calculations of exotic molecules, where other force field have not been created.

### 3.3.2 Assisted Model Building with Energy Refinement (AMBER)

AMBER is both a molecular dynamics package and a set of force fields [11, 17]. The force field uses 12-6 Lennard-Jones, equation 3.2.9, with parameters computed by Lorentz-Berthelot mixing rules, equations 3.2.10 and 3.2.11, 1-4 interactions are scaled by $\frac{1}{2}$ and

Columbic interactions are represented by point charges and are scaled by $\frac{5}{6}$. Bond and angle interactions are expressed as harmonic potentials and torsional interactions are represented as a cosine series.

AMBER force fields are all atom only (though the newest force field, ff12sb, does include some united atom parameter), parametrised for biomolecular simulations and contains the 20 common amino acids as functional groups. More recently there have been some work put in to extend the AMBER force field to a wider range of systems through the development of the general AMBER force field (GAFF)[18].

### 3.3.3 Chemistry at HARvard Molecular Mechanics (CHARMM)

CHARMM is also molecular dynamics program [10], as well as a set of force fields. There are all atom CHARMM22 [19, 20], CHARMM27 [21], CgenFF [22], and united atom CHARMM19 [23] force fields. The potential function is of the same form as AMBER; however, non-bonded parameters are not scaled.

All of the force fields, apart from more recent CgenFF, were parametrised for biomolecular simulations, similarly to AMBER, containing the 20 common amino acid groups. CgenFF was created as a general force field for drug-type molecules, to accompany the rest of the force fields.

### 3.3.4 Optimised Potentials for Liquid Simulations (OPLS)

OPLS force field was developed by group of William L. Jorgensen and contains several sets of parameters, for both all atom and united atom calculations that can be mixed [9, 13]. The potential functions are the same as in AMBER, Lennard-Jones is computed by geometrical mean mixing rules, equation 3.2.12. Both, Lennard-Jones and Coulombic, parameters are scaled by a $1/2$.

OPLS at the beginning was parametrised not only for biomolecular systems, but also organic liquids. The parameters were optimized to fit experimental densities and heats of vaporisation of liquids, as well as gas-phase torsional profiles. The force field has being updated and many independent modifications to the force field have been developed [24, 25]. OPLS is, arguably, the most widely parametrised force field available.

### 3.3.5 GROningen MOlecular Simulation (GROMOS)

GROMOS is also both a molecular dynamics package [14] and the complementary force field. The first was also the base for GROMACS package [26]. GROMOS is a united atom force field, with ongoing improvements being done, currently most widely used version of the force field is GROMOS-96 [27] and its latest update [28]. This force field is also aimed at biomolecular calculations and is parametrised for proteins.

Unlike AMBER, the Lennard-Jones parameters for heteroatomic interactions are readily provided by the force field and should not be calculated via mixing rules. The force field uses a quartic expression for the bond length, a harmonic cosine potential for angle bending and a single cosine series for torsional angle potential.

### 3.3.6 Transferable Potentials for Phase Equilibria (TraPPE)

TraPPE force field evolved from the previous SKS (Smit-Karaborni-Siepmann) force field [**?** ]. SKS was developed in Shell laboratories in the 1990s and is the first force field, aimed at reproducing properties of $n$-alkanes, the main components in fuels. The TraPPE

force field contains parameters for alkanes, aromatics, some oxygen, sulphur and nitrogen containing compounds.

TraPPE force field is mainly united atom [15, 29–34] with two explicit hydrogen models [35, 36]. Unlike most of united atom force fields, in TraPPE hydrogen atoms are also united in aromatic interactions.

The functional form is the same as in AMBER, including mixing rules, Coulombic terms are scaled by a $\frac{1}{2}$. Since the force field was developed with Monte Carlo calculations, there is no improper torsional angle term what can lead to incorrect conformations when performing molecular dynamics. The force field is parametrised to fit the vapour-liquid coexistence curve for small organic molecules.

## 3.4 Water Models

Water molecular models have been developed in order to help discover the structure of water. They are useful given the basis that if the (known but hypothetical) model can successfully predict the physical properties of liquid water then the (unknown) structure of liquid water is determined. There are two general forms for these models of water:

**Explicit Water,** where each water molecule is simulated directly.

**Implicit Water,** where the general effects of water are taken into account but the molecules are not directly simulated.

### 3.4.1 Explicit Water

When simulating water explicitly it is important to use an accurate but efficient model. This is due to the computational expensiveness of simulating water in a solvated system, e.g. in simulating a protein in periodic box full of water at aqueous density about 90% of the computational time is used in simulating water-water interactions.

The original atomic-scale computational model for liquid water was proposed by Bernal and Fowler in 1933 [37]. This model took into account the position and the charge on the hydrogens and the position of the negative charge in the molecule. It was a highly insightful model and similar to the general view in Figure 3.8(c). At the time of the earliest developments of protein force fields the ST2 model of Stillinger and Rahman [38] was in wide use, which lead to the ST2 model being for some of the first protein simulations.

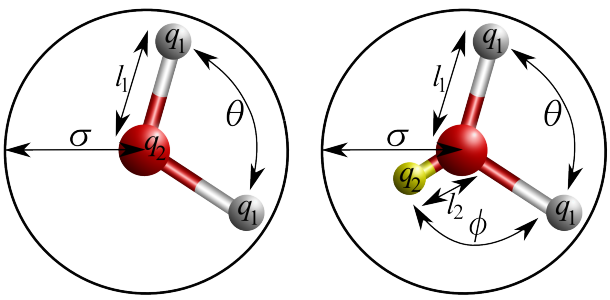


(a) 3-site




(b) 4-site

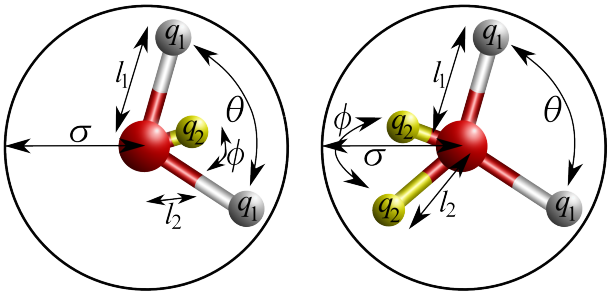


In the early 1980s two new force fields were developed, the SPC [39] and TIP3P [40] models. They involve orienting electrostatic effects and Lennard-Jones sites. The Lennard-Jones interaction accounts for the size of the molecules. It is repulsive at short distances, a ensuring that the structure does not completely collapse due to the electrostatic interactions. At intermediate distances it is significantly attractive but non-directional and competes with the directional attractive electrostatic interactions.

This competition ensures a tension between an expanded tetrahedral network and a collapsed non-directional network (for example, similar to that found in liquid noble gases).

Since then many models for water have been created around these general principles, although the charge and Lennard-Jones sites don't always coincide. The four main general model types are shown in Figure 3.8. Generally each model is developed to fit well with one particular physical structure or parameter (for example, the density anomaly, radial distribution function or the critical parameters) and it comes as no surprise when a model developed to fit certain parameters it gives good compliance with these same parameters [41]. In spite of the heavy computational investment in the calculations, the final agreement with experimental data is often 'by eye' and not statistically tested or checked for parametric sensitivity. Also, tests for 'quality' often use the radial distribution fit with diffraction data in spite of the major fitted peaks being derived from the tetrahedral nature of water that is built into every model and overpowers any disagreement in the fine detail. In particular, the O—O radial distribution function seems to be a poor discriminator between widely differently performing models [42]. Table 3.1 shows the values predicted for some key water properties by some of the most popular water force fields.

### 3.4.2 Implicit Water

There are many circumstances in molecular modeling studies in which a simplified description of solvent effects has advantages over the explicit modelling of each solvent molecule. Most of these are where the saving of computer time are needed over using explicit water. Most of the simulation techniques have models in which the solute degrees of freedom are treated explicitly but the solvent degrees of freedom are not. This requires that the energy surface used for the protein degrees of freedom be a potential of mean force (PMF) in which the solvent degrees of freedom are implicitly averaged over [66]. Assuming that the full potential energy function consists of a term, $U_{\text{vac}}$ for the interactions within the protein, depending only on the protein degrees of freedom, $\mathbf{r}$, and an additional term for the protein-solvent and solvent-solvent interactions, the PMF is ideally equation 3.4.1, where $DeltaG_{\text{sol}}(\mathbf{r})$ is the free energy of transferring the protein from vacuum to the solvent with its internal degrees of freedom fixed at $\mathbf{r}$.

$$U_{\text{PMF}}(\mathbf{r}) = U_{\text{vac}}(\mathbf{r}) + \Delta G_{\text{sol}}(\mathbf{r}) \tag{3.4.1}$$

Some of the main models are:

**COSMO Model** [67] treats the solvent as a high dielectric continuum, interacting with charges that are embedded in solute molecules of lower dielectric. In spite of the severity of the approximation, this model often gives a good account of equilibrium solvation energetics.

**Poisson-Boltzmann Model** [68] describes electrostatic interactions in a multiple-dielectric environment and are typically solved by finite-difference or boundary element numerical methods. These can be efficiently solved for small molecules but may become expensive for proteins or nucleic acids. Although progress continues to be

made in numerical solutions, there is a clear interest in exploring more efficient, if approximate, approaches to this problem.

**Generalized Born Model** [69, 70] computes the electrostatic work required to move a charged sphere from a vacuum environment into a continuous dielectric region. The result is proportional to the square of the charge and is inversely proportional to the size of the ion. The basis of generalized Born theory is to extend these ideas to non-spherical molecules by casting the electrostatic contribution to solvation. The Born model have not traditionally considered salt effects, but the model has be extended to low-salt concentrations [71]. The key to making Generalized Born calculations more accurate (in the sense of agreement with Poisson-Boltzmann calculations) is improved estimation of the effective Born radii [72].

Table 3.1: Calculated physical properties of the water models at 25 °C and 1 atm.

| Model | Type | Dipole Moment | Dielectric constant | Self Diffusion / $10^{-5}$cm$^2$ s$^{-1}$ | Average Configurational Energy / kJ mol$^{-1}$ | Density Maximum Temperature /°C | Expansion Coefficient, $10^{-4}$ °C$^{-1}$ |
|---|---|---|---|---|---|---|---|
| SSD [43] | -[1] | 2.35 [43] | 72 [43] | 2.13 [43] | -40.2 [43] | -13 [43] | - |
| SPC [39] | a | 2.27 [44] | 65 [45] | 3.85 [46] | -41.0 [45] | -45 [47] | 7.3[2][48] |
| SPC/E [49] | a | 2.35 [49] | 71 [49] | 2.49 [46] | -41.5 [49] | -38 [50] | 5.14 [51] |
| SPC/Fw[4][51] | a | 2.39 [51] | 79.63 [51] | 2.32 [51] | - | - | 4.98 [51] |
| PPC[4][49] | b | 2.52 [49] | 77 [49] | 2.6 [49] | -43.2 [49] | 4 [52] | - |
| TIP3P [40] | a | 2.35 [53] | 82 [49] | 5.19 [46] | -41.1 [53] | -91 [47] | 9.2 [53] |
| TIP3P/Fw[4][51] | a | 2.57 [51] | 193 [51] | 3.53 [51] | - | - | 7.81 [51] |
| TIP4P [53] | c | 2.18 [49, 53] | 53 [49] | 3.29 [46] | -41.8 [53] | -25 [53] | 4.4 [53] |
| TIP4P-Ew [54] | c | 2.32 [54] | 62.9 [54] | 2.4 [54] | -46.5 [54] | 1 [54] | 3.1 [54] |
| TIP4P-FQ [55] | c | 2.64 [55] | 79 [55] | 1.93 [55] | -41.4 [56] | 7 [55] | - |
| TIP4P/2005 [41] | c | 2.305 [41] | 60 [41] | 2.08 [41] | - | 5 [41] | 2.8 [41] |
| TIP4P/2005f [57] | c | 2.319 [57] | 55.3 [57] | 1.93 [57] | - | 7 [57] | - |
| SWFLEX-AI[4][56] | c | 2.69 [56] | 116 [56] | 3.66 [56] | -41.7 [56] | - | - |
| COS/G3 [48] | c | 2.57[2][48] | 88[2][48] | 2.6[2][48] | -41.1[2][48] | - | 7.0[2][48] |
| COS/D [58] | c | 2.43 [58] | 69.8 [58] | 2.5 [58] | -41.8 [58] | - | - |
| GCPM[4][59] | c | 2.723 [59] | 84.3 [59] | 2.26 [59] | -44.8 [59] | -13 [59] | - |
| SWM4-NDP[4][60] | c | 2.461 [60] | 79 [60] | 2.33 [60] | -41.5 [60] | - | - |
| TIP5P [53] | d | 2.29 [53] | 81.5 [53] | 2.62 [46] | -41.3 [53] | 4 [53] | 6.3 [53] |
| TIP5P-Ew [61] | d | 2.29 [61] | 92 [61] | 2.8 [61] | - | 8 [61] | 4.9 [61] |
| TTM2-F [62] | c | 2.67 [62] | 67.2 [62] | 1.4 [62] | -45.1 [62] | - | - |
| POL5/TZ[4][63] | d | 2.712 [63] | 98 [63] | 1.81 [63] | -41.5 [63] | 25 [63] | - |
| Six-site [64] | c+d | 1.89[3][64] | 33[3][64] | - | - | 14[3][64] | 2.4[3][64] |
| QCT [65] | a | 1.85[2][65] | - | 1.5[2][65] | -42.7[2][65] | 10[2][65] | 3.5[2][65] |
| Experimental | - | 2.95 | 78.4 | 2.30 | -41.5 [53] | 3.984 | 2.53 |

[1]Has only a single, center of mass, interaction site with a tetrahedrally coordinated sticky potential that regulates the tetrahedral coordination of neighboring molecules

[2]Calculated at 27 °C

[3]Calculated at 20 °C

[4]Polarizable model

## 3.5 Coarse-Graining

Even though computational power is rapidly increasing, with hardware performance doubling every two years [73] (technically the number of transistors doubling), coupled to the development of ever more efficient algorithms to deliver faster and more accurate calculations; there is a pressing need to simulate chemical systems over timescales that go far beyond those currently obtainable with atomistic systems.

The basic concept of coarse graining involves a reduction of the number of sites in a system. This not only allows for smaller computational load, but also leads to a loss of fine detail in the system. There has to be a delicate balance between these two things, ideally leading to a considerable speed up of the calculation while still preserving the necessary chemical and physical information. Decreasing the number of the interaction sites in a model allows a significant speed up in the calculation. Computer time approximately scales as $N^2$ ($N$ is a number of interaction sites) for pairwise potentials. Additionally, some intermolecular movements are lost, allowing the system to explore phase space faster. A third speed up is due to the increase of time step for the calculation, as the vibration frequency of larger particles is slower.

In chemistry, a coarse grained system will typically still be represented at the molecular level, as prediction of local properties of the system is dependent on the presence of molecules. A common type of coarse grained model represents of a group of atoms with a single interaction centre, a so called "super atom". These super atoms are then assigned interaction parameters. The parameters are derived from a smaller scale, higher resolution model of the system. Additionally, they may be fitted to the experimental values. Results of the calculation are dependant on them, so care should be taken when parametrizing the system.

Currently there is only one readily available coarse grained force field, MARTINI [74]. The force field is designed to be used in biomolecular simulations of lipids, proteins and carbohydrates [75–77]. The model uses a shifted Lennard-Jones 12-6 potential with parameters fitted to free energies of vaporisation, hydration and separation between water and organic solvents at room (300 K) temperature only. There are criticisms of water in this model due to its inability to remain in the liquid state in membrane pores [78, 79]. Recently a more sophisticated, polarizable water model was developed by the same group [80]. Water is proving to be one of the most difficult systems to coarse grain, as finding potentials capable of exhibiting the correct behaviour is difficult; though several efforts have been made recently [81–83].

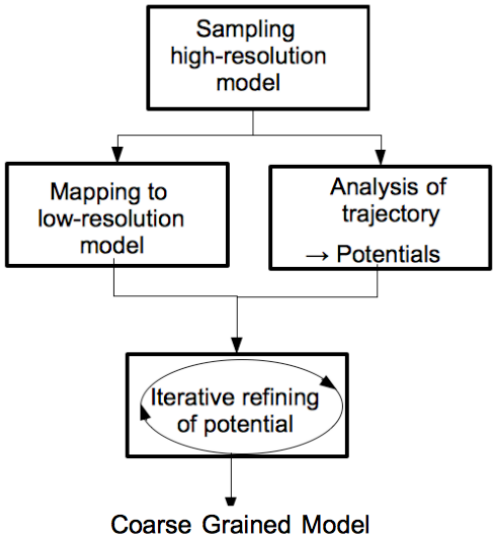


Figure 3.9: Illustration of the coarse graining procedure: sampling of a high resolution model, analysis of the trajectory, mapping to low resolution, iterative refining of the potential.

The main constraint of coarse grained potentials is the limited transferability between different systems and thermodynamic conditions. Transferability is highly dependent on the system parametrised, and is generally better for finer grained models; for polymer systems transferability is not greatly affected by a change in the length of the polymer chain [84].

To derive a suitable coarse grain potential, one would normally follow the general procedure, shown in the Figure 3.9. A smaller scale, higher resolution atomistic (sometimes united-atom) model is sampled using molecular dynamics or Monte Carlo simulations. When setting up the initial calculation and then mapping the system, it is important consider which properties are needed and at which time and length scales. The trajectories from high resolution calculation are then analysed and the starting potentials for the coarse grain model are obtained. For most of the cases it is necessary to refine the latter to obtain consistent results with the higher resolution method.

### 3.5.1 Mapping

In the mapping procedure, one represents a group of atoms with a single interaction centre. This centre is called a super atom and commonly positioned at the centre of mass of the group of initial atoms. Super atoms, as in atomistic calculations, are interlinked with springs and follow the same rules of Newtonian mechanics. The choice of atoms to group into a bead is typically done by geometrical examination of the molecule and leads to a coarse grained molecule still resembling the general shape of the initial molecule. This will allow a better agreement of non bonded properties. Additionally, one should consider which interactions form the simplest, if possible single well or simple shape potentials, that will be beneficial in refining the system in further iterative steps [85]. The parts of the molecule that are geometrically mobile (eg. undergoing gauche–trans conformational changes) will typically lead to potentials with more then one well.

### 3.5.2 Potentials

When the mapping is chosen, the next step is to evaluate the optimum parameters to describe the interactions between the coarse grained sites. Over the last few years a number of approaches have been developed:

**Force matching** , where a multibody potential of mean force of a high resolution system is matched by a low resolution one [86]. This approach looks at individual configurations, rather than the average properties of the system as encompassed by radial distribution functions [87, 88].

**Inverse Monte Carlo** , where the new parameters are fitted by the use of Monte Carlo calculations [89, 90]. The potentials are derived from distributions, e.g.% bond length, angle, dihedral angle, and radial distribution functions.

**Iterative Boltzmann Inversion** , where the new parameters are fitted with the aid of molecular dynamics calculations [91]. The potentials are derived from distributions, e.g. bond length, angle, dihedral angle, and radial distribution functions.

### 3.5.3 Iterative Boltzmann Inversion

Iterative Boltzmann Inversion is a structure based method and is aimed at matching distribution functions of a new coarse grained model to a higher resolution calculation or experiment. Bonded interactions (bond, angle and dihedral) incorporate neglected degrees of freedom and temperature effects. Non-bonded are calculated separately, creating physically sensible interactions between molecules. Generally, bonded potentials are stronger than non bonded ones. The fitting of the potentials should start with the strongest one

(deepest potential well), as it will change the least during fitting of the rest, hence the order:

$$P_{bond} \rightarrow P_{angle} \rightarrow P_{dihedral} \rightarrow P_{nonbonded}$$

Figure 3.10 illustrates the procedure for deriving an effective potential $V(x)$ from a known probability distribution, $P_{ref}(x)$. $P(x)$ is a general term for the distribution, that could be a radial distribution function, $g(r)$; bond length, $b(r)$; angle, $a(\theta)$; or dihedral angle, $d(\phi)$; distribution.

For the first step of the iteration, a reasonable guess of an effective potential should be obtained. This can be derived from a reference probability, $P_{ref}(x)$, of a high resolution simulation of a pure system, equation 3.5.1.

$$V_0(\mathbf{x}) = -k_B T \ln P_{ref}(\mathbf{x}) \qquad (3.5.1)$$

It should be mentioned that $V_0$ is not a potential energy, but rather a free energy, dependant on temperature and pressure. $V_0$ is a reasonable guess for the first coarse grained potential. A coarse grained simulation is performed and new probability distributions $P_i(\mathbf{x})$ evaluated. The new distribution will differ from $P_{ref}(\mathbf{x})$ and so the new potential should include a correction, in order to provide a better representation of the system equation 3.5.2 is used, where $\lambda$ is a numerical scaling factor and should be $\lambda \in (0, 1]$.

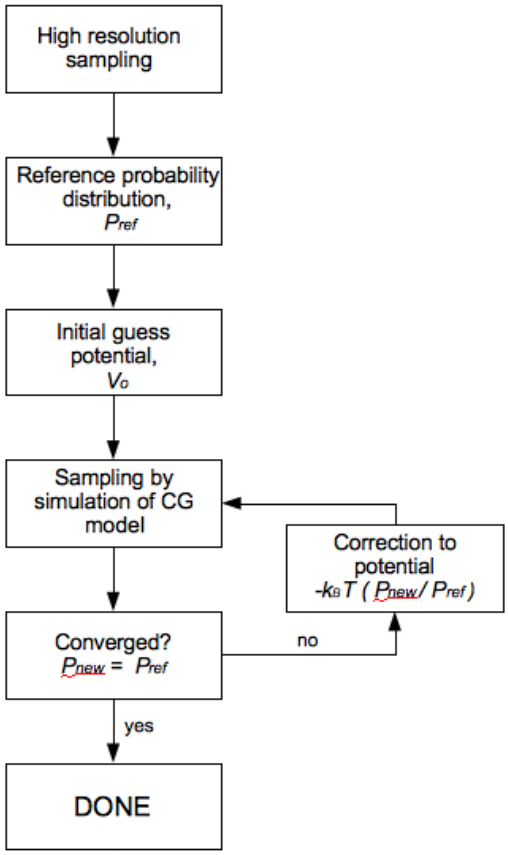


Figure 3.10: Illustrated procedure for deriving effective potentials by the iterative Boltzmann inversion (IBI) method.

$$V_{i+1}(\mathbf{x}) = V_i(\mathbf{x}) - \lambda k_B T \ln \frac{P_i(\mathbf{x})}{P_{ref}(\mathbf{x})} \qquad (3.5.2)$$

The new calculation will again result in a probability distribution, $P_{i+1}$. The iterative procedure should be repeated until $P_{i+n}$ is sufficiently close to $P_{ref}$. It has been tested by numerous authors and shown that it can take up to 200 iterations to obtain a potential capable of representing aggregate distributions [92] and over 1000 iterations to recover correct potential functions [93].

## 3.6 References

[1] Philip M. Morse. Diatomic Molecules According to the Wave Mechanics. II. Vibrational Levels. *Phys. Rev.*, 34:57–64, Jul 1929.

[2] Gustav Mie. Zur kinetischen Theorie der einatomigen KÃűrper. *Annalen der Physik*, 316(8):657–697, 1903.

[3] A. Warshel and S. Lifson. Consistent force field calculations. II. Crystal structures, sublimation energies, molecular and lattice vibrations, molecular conformations, and enthalpies of alkanes. *The Journal of Chemical Physics*, 53:582, 1970.

[4] David N.J. White. A computationally efficient alternative to the Buckingham potential for molecular mechanics calculations. *Journal of Computer-Aided Molecular Design*, 11:517–521, 1997. 10.1023/A:1007911511862.

[5] J. E. Jones. On the Determination of Molecular Fields. I. From the Variation of the Viscosity of a Gas with Temperature. *Proceedings of the Royal Society of London. Series A*, 106(738):441–462, 1924.

[6] H. A. Lorentz. Ueber die Anwendung des Satzes vom Virial in der kinetischen Theorie der Gase. *Annalen der Physik*, 248(1):127–136, 1881.

[7] Robert J. Good and Christopher J. Hope. New Combining Rule for Intermolecular Distances in Intermolecular Potential Functions. *The Journal of Chemical Physics*, 53(2):540–543, 1970.

[8] B. E. F. Fender and Jr. G. D. Halsey. Second Virial Coefficients of Argon, Krypton, and Argon-Krypton Mixtures at Low Temperatures. *The Journal of Chemical Physics*, 36(7):1881–1888, 1962.

[9] William L. Jorgensen, David S. Maxwell, and Julian Tirado-Rives. Development and Testing of the OPLS All-Atom Force Field on Conformational Energetics and Properties of Organic Liquids. *Journal of the American Chemical Society*, 118(45):11225–11236, 1996.

[10] B. R. Brooks, C. L. Brooks, A. D. Mackerell, L. Nilsson, R. J. Petrella, B. Roux, Y. Won, G. Archontis, C. Bartels, S. Boresch, A. Caflisch, L. Caves, Q. Cui, A. R. Dinner, M. Feig, S. Fischer, J. Gao, M. Hodoscek, W. Im, K. Kuczera, T. Lazaridis, J. Ma, V. Ovchinnikov, E. Paci, R. W. Pastor, C. B. Post, J. Z. Pu, M. Schaefer, B. Tidor, R. M. Venable, H. L. Woodcock, X. Wu, W. Yang, D. M. York, and M. Karplus. CHARMM: The biomolecular simulation program. *Journal of Computational Chemistry*, 30(10):1545–1614, 2009.

[11] Wendy D. Cornell, Piotr Cieplak, Christopher I. Bayly, Ian R. Gould, Kenneth M. Merz, David M. Ferguson, David C. Spellmeyer, Thomas Fox, James W. Caldwell, and Peter A. Kollman. A Second Generation Force Field for the Simulation of Proteins, Nucleic Acids, and Organic Molecules. *Journal of the American Chemical Society*, 117(19):5179–5197, 1995.

[12] A. K. Rappe, C. J. Casewit, K. S. Colwell, W. A. Goddard, and W. M. Skiff. UFF, a full periodic table force field for molecular mechanics and molecular dynamics simulations. *Journal of the American Chemical Society*, 114(25):10024–10035, 1992.

[13] William L. Jorgensen and Julian. Tirado-Rives. The OPLS [optimized potentials for liquid simulations] potential functions for proteins, energy minimizations for crystals of cyclic peptides and crambin. *Journal of the American Chemical Society*, 110(6):1657–1666, 1988.

[14] Markus Christen, Philippe H. Hunenberger, Dirk Bakowies, Riccardo Baron, Roland Burgi, Daan P. Geerke, Tim N. Heinz, Mika A. Kastenholz, Vincent Krautler, Chris Oostenbrink, Christine Peter, Daniel Trzesniak, and Wilfred F. van Gunsteren. The

GROMOS software for biomolecular simulation: GROMOS05. *Journal of Computational Chemistry*, 26(16):1719–1751, 2005.

[15] M.G. Martin and J.I. Siepmann. Transferable potentials for phase equilibria. 1. United-atom description of n-alkanes. *The Journal of Physical Chemistry B*, 102(14):2569–2577, 1998.

[16] Marcus G. and Martin. Comparison of the AMBER, CHARMM, COMPASS, GROMOS, OPLS, TraPPE and UFF force fields for prediction of vaporâĂŞliquid coexistence curves and liquid densities. *Fluid Phase Equilibria*, 248(1):50 – 55, 2006.

[17] Yong Duan, Chun Wu, Shibasish Chowdhury, Mathew C. Lee, Guoming Xiong, Wei Zhang, Rong Yang, Piotr Cieplak, Ray Luo, Taisung Lee, James Caldwell, Junmei Wang, and Peter Kollman. A point-charge force field for molecular mechanics simulations of proteins based on condensed-phase quantum mechanical calculations. *Journal of Computational Chemistry*, 24(16):1999–2012, 2003.

[18] Junmei Wang, Romain M. Wolf, James W. Caldwell, Peter A. Kollman, and David A. Case. Development and testing of a general amber force field. *Journal of Computational Chemistry*, 25(9):1157–1174, 2004.

[19] A. D. MacKerell, D. Bashford, Bellott, R. L. Dunbrack, J. D. Evanseck, M. J. Field, S. Fischer, J. Gao, H. Guo, S. Ha, D. Joseph-McCarthy, L. Kuchnir, K. Kuczera, F. T. K. Lau, C. Mattos, S. Michnick, T. Ngo, D. T. Nguyen, B. Prodhom, W. E. Reiher, B. Roux, M. Schlenkrich, J. C. Smith, R. Stote, J. Straub, M. Watanabe, J. Wiorkiewicz-Kuczera, D. Yin, and M. Karplus. All-Atom Empirical Potential for Molecular Modeling and Dynamics Studies of ProteinsâĂă. *The Journal of Physical Chemistry B*, 102(18):3586–3616, 1998.

[20] A.D. Mackerell Jr, M. Feig, and C.L. Brooks III. Extending the treatment of backbone energetics in protein force fields: Limitations of gas-phase quantum mechanics in reproducing protein conformational distributions in molecular dynamics simulations. *Journal of computational chemistry*, 25(11):1400–1415, 2004.

[21] A.D. MacKerell Jr, N. Banavali, and N. Foloppe. Development and current status of the CHARMM force field for nucleic acids. *Biopolymers*, 56(4):257–265, 2000.

[22] K. Vanommeslaeghe, E. Hatcher, C. Acharya, S. Kundu, S. Zhong, J. Shim, E. Darian, O. Guvench, P. Lopes, I. Vorobyov, et al. CHARMM general force field: A force field for drug-like molecules compatible with the CHARMM all-atom additive biological force fields. *Journal of computational chemistry*, 31(4):671–690, 2010.

[23] III WH Reiher. *Theoretical studies of hydrogen bonding*. PhD thesis, Harvard University, 1985.

[24] S.V. Sambasivarao and O. Acevedo. Development of OPLS-AA force field parameters for 68 unique ionic liquids. *Journal of Chemical Theory and Computation*, 5(4):1038–1050, 2009.

[25] Z. Xu, H.H. Luo, and D.P. Tieleman. Modifying the OPLS-AA force field to improve hydration free energies for several amino acid side chains using new atomic charges and an off-plane charge model for aromatic residues. *Journal of computational chemistry*, 28(3):689–697, 2007.

[26] Berk Hess, Carsten Kutzner, David van der Spoel, and Erik Lindahl. GROMACS 4: Algorithms for Highly Efficient, Load-Balanced, and Scalable Molecular Simulation. *Journal of Chemical Theory and Computation*, 4(3):435–447, 2008.

[27] Wilfred F. van Gunsteren, S. R. Billeter, A. A. Eising, Philippe H. Hünenberger, P. Krüger, Alan E. Mark, W. R. P. Scott, and Ilario G. Tironi. *Biomolecular Simulation: The GROMOS96 manual and user guide*. 1996.

[28] Markus Christen, Philippe H. HÃijnenberger, Dirk Bakowies, Riccardo Baron, Roland BÃijrgi, Daan P. Geerke, Tim N. Heinz, Mika A. Kastenholz, Vincent Krautler, Chris Oostenbrink, Christine Peter, Daniel Trzesniak, and Wilfred F. van Gunsteren. The GROMOS software for biomolecular simulation: GROMOS05. *Journal of Computational Chemistry*, 26(16):1719–1751, 2005.

[29] M.G. Martin and J.I. Siepmann. Novel configurational-bias Monte Carlo method for branched molecules. Transferable potentials for phase equilibria. 2. United-atom description of branched alkanes. *The Journal of Physical Chemistry B*, 103(21):4508–4517, 1999.

[30] C.D. Wick, M.G. Martin, and J.I. Siepmann. Transferable potentials for phase equilibria. 4. United-atom description of linear and branched alkenes and alkylbenzenes. *The Journal of Physical Chemistry B*, 104(33):8008–8016, 2000.

[31] B. Chen, J.J. Potoff, and J.I. Siepmann. Monte Carlo calculations for alcohols and their mixtures with alkanes. Transferable potentials for phase equilibria. 5. United-atom description of primary, secondary, and tertiary alcohols. *The Journal of Physical Chemistry B*, 105(15):3093–3104, 2001.

[32] J.M. Stubbs, J.J. Potoff, and J.I. Siepmann. Transferable potentials for phase equilibria. 6. United-atom description for ethers, glycols, ketones, and aldehydes. *The Journal of Physical Chemistry B*, 108(45):17596–17605, 2004.

[33] C.D. Wick, J.M. Stubbs, N. Rai, and J.I. Siepmann. Transferable potentials for phase equilibria. 7. Primary, secondary, and tertiary amines, nitroalkanes and nitrobenzene, nitriles, amides, pyridine, and pyrimidine. *The Journal of Physical Chemistry B*, 109(40):18974–18982, 2005.

[34] N. Lubna, G. Kamath, J.J. Potoff, N. Rai, and J.I. Siepmann. Transferable potentials for phase equilibria. 8. United-atom description for thiols, sulfides, disulfides, and thiophene. *The Journal of Physical Chemistry B*, 109(50):24100–24107, 2005.

[35] B. Chen and J.I. Siepmann. Transferable potentials for phase equilibria. 3. Explicit-hydrogen description of normal alkanes. *The Journal of Physical Chemistry B*, 103(25):5370–5379, 1999.

[36] N. Rai and J.I. Siepmann. Transferable potentials for phase equilibria. 9. Explicit hydrogen description of benzene and five-membered and six-membered heterocyclic aromatic compounds. *The Journal of Physical Chemistry B*, 111(36):10790–10799, 2007.

[37] J. D. Bernal and R. H. Fowler. A Theory of Water and Ionic Solution, with Particular Reference to Hydrogen and Hydroxyl Ions. *Journal of Chemical Physics*, 1:515–548, 1933.

[38] F. H. Stillinger and A. Rahman. Improved simulation of liquid water by molecular dynamics. *Journal of Chemical Physics*, 60:1545–1557, 1974.

[39] H. J. C. Berendsen, J. P. M. Postma, W. F. van Gunsteren, and J. Hermans. *Intermolecular Forces*. Reidel, Dordrecht, 1981.

[40] W. L. Jorgensen, J. Chandrasekhar, J. D. Madura, R. W. Impey, and M. L. Klein. Comparison of simple potential functions for simulating liquid water. *Journal of Chemical Physics*, 79:926–935, 1983.

[41] J. L. F. Abascal and C. Vega. A general purpose model for the condensed phases of water: TIP4P/2005. *Journal of Chemical Physics*, 123:234505, 2005.

[42] P. E. Mason and J. W. Brady. "Tetrahedrality" and the relationship between collective structure and radial distribution functions in liquid water. *Journal of Physical Chemistry B*, 111:5669–5679, 2007.

[43] M-L. Tan, J. T. Fischer, A. Chandra, B. R. Brooks, and T.ÂăIchiye. A temperature of maximum density in soft sticky dipole water. *Chemical Physics Letters*, 376:646–652, 2003.

[44] K. Kiyohara, K. E. Gubbins, and A. Z. Panagiotopoulos. Phase coexistence properties of polarizable water models. *Molecular Physics*, 94:803–808, 1998.

[45] D. van der Spoel, P. J. van Maaren, and H. J. C. Berendsen. A systematic study of water models for molecular simulation: Derivation of water models optimized for use with a reaction field. *Journal of Chemical Physics*, 108:10220–10230, 1998.

[46] M. W. Mahoney and W. L. Jorgensen. Diffusion constant of the TIP5P model of liquid water. *Journal of Chemical Physics*, 114:363–366, 2001.

[47] C. Vega and J. L. F. Abascal. Relation between the melting temperature and the temperature of maximum density for the most common models of water. *Journal of Chemical Physics*, 123:144504, 2005.

[48] H. Yu and W. F. van Gunsteren. Charge-on-spring polarizable water models revisited: from water clusters to liquid water to ice. *Journal of Chemical Physics*, 121:9549–9564, 2004.

[49] H. J. C. Berendsen, J. R. Grigera, and T. P. Straatsma. The missing term in effective pair potentials. *Journal of Physical Chemistry*, 91:6269–6271, 1987.

[50] L. A. Baez and P. Clancy. Existence of a density maximum in extended simple point-charge water. *Journal of Chemical Physics*, 101:9837–9840, 1994.

[51] Y. Wu, H. L. Tepper, and G. A. Voth. Flexible simple point-charge water model with improved liquid state properties. *Journal of Chemical Physics*, 124Âă:024503, 2006.

[52] I. M. Svishchev, P. G. Kusalik, J. Wang, and R. J. Boyd. Polarizable point-charge model for water. Results under normal and extreme conditions. *Journal of Chemical Physics*, 105:4742–4750, 1996.

[53] M. W. Mahoney and W. L. Jorgensen. A five-site model for liquid water and the reproduction of the density anomaly by rigid, nonpolarizable potential functions. *Journal of Chemical Physics*, 112:8910–8922, 2000.

[54] H. W. Horn, W. C. Swope, J. W. Pitera, J. D. Madura, T. J. Dick, G. L. Hura, and T. Head-Gordon. Development of an improved four-site water model for biomolecular simulations. *Journal of Chemical Physics*, 120:9665–9678, 2004.

[55] S. W. Rick. Simulation of ice and liquid water over a range of temperatures using the fluctuating charge model. *Journal of Chemical Physics*, 114:2276–2283, 2001.

[56] P. J. van Maaren and D. van der Spoel. Molecular dynamics of water with novel shell-model potentials. *Journal of Physical Chemistry B*, 105:2618–2626, 2001.

[57] M. A. González and J. L. F. Abascal. A flexible model for water based on TIP4P/2005. *Journal of Chemical Physics*, 135:224516, 2011.

[58] A.-P. E. Kunz and W. F. van Gunsteren. Development of a nonlinear classical pPolarization model for liquid water and aqueous solutions: COS/D. *Journal of Physical Chemistry A*, 113:11570–11579, 2009.

[59] P. Paricaud, M. Predota, A. A. Chialvo, and P. T. Cummings. From dimer and condensed phases at extreme conditions: Accurate predictions of the properties of water by a Gaussian charge polarizable model. *Journal of Chemical Physics*, 122:244511, 2005.

[60] G. Lamoureux, E. Harder, I. V. Vorobyov, B. Roux, and A. D. MacKerell Jr. A polarizable model of water for molecular dynamics simulations of biomolecules. *Chemical Physics Letters*, 418:241–245, 2005.

[61] S. W. Rick. A reoptimization of the five-site water potential (TIP5P) for use with Ewald sums. *Journal of Chemcal Physics*, 120:6085–6093, 2004.

[62] G. S. Fanourgakis and S. S. Xantheas. The flexible, polarizable, Thole-type interaction potential for water (TTM2-F) revisited. *Journal of Physical Chemistry A*, 110:4100–4106, 2006.

[63] H. A. Stern, F. Rittner, B. J. Berne, and R. A. Friesner. Combined fluctuating charge and polarizable dipole models: Application to a five-site water potential function. *Journal of Chemical Physics*, 115:2237–2251, 2001.

[64] H. Nada and J. P. J. M. van der Eerden. An intermolecular potential model for the simulation of ice and water near the melting point: A six-site model of $H_2O$. *Journal of Chemical Physics*, 118:7401–7413, 2003.

[65] S. Y. Liem, P. L. A. Popelier, and M. Leslie. Simulation of liquid water using a high-rank quantum topological electrostatic potential. *International Journal of Quantum Chemistry*, 99:685–694, 2004.

[66] B Roux and T. Simonson. *Biophysical Chemistry*, 78:1–20, 1999.

[67] A. Klamt and G. Schüürmann. *J Chem. Soc. Perkin Trans*, 2:799–805, 1993.

[68] C. J. Cramer and D. G. Truhlar. *Chemical Reviews*, 99:2161–2200, 1999.

[69] M. Born. *Z. Phys.*, 1:45–48, 1920.

[70] D. Bashford and D. Case. *Annu. Rev. Phys. Chem.*, 51:129–152, 2000.

[71] J. Srinivasan, M. W. Trevathan, P. Beroza, and D. A. Case. *Theor. Chem. Ace.*, 101:126–434, 1999.

[72] M. S. Lee, F. R. Salsbury Jr, and C. L. Brooks III. *Journal of Physical Chemistry*, 116,:10606–10614, 2002.

[73] G. E. Moore. Cramming more components onto integrated circuits. *Electronics*, 38:114–117, 1965.

[74] S.J. Marrink, A.H. de Vries, and A.E. Mark. Coarse grained model for semiquantitative lipid simulations. *The Journal of Physical Chemistry B*, 108(2):750–760, 2004.

[75] S.J. Marrink, H.J. Risselada, S. Yefimov, D.P. Tieleman, and A.H. De Vries. The MARTINI force field: coarse grained model for biomolecular simulations. *The Journal of Physical Chemistry B*, 111(27):7812–7824, 2007.

[76] L. Monticelli, S.K. Kandasamy, X. Periole, R.G. Larson, D.P. Tieleman, and S.J. Marrink. The MARTINI coarse-grained force field: extension to proteins. *Journal of Chemical Theory and Computation*, 4(5):819–834, 2008.

[77] C.A. López, A.J. Rzepiela, A.H. de Vries, L. Dijkhuizen, P.H. Hünenberger, and S.J. Marrink. Martini coarse-grained force field: extension to carbohydrates. *Journal of Chemical Theory and Computation*, 5(12):3195–3210, 2009.

[78] M. Winger, D. Trzesniak, R. Baron, and W.F. Van Gunsteren. On using a too large integration time step in molecular dynamics simulations of coarse-grained molecular models. *Phys. Chem. Chem. Phys.*, pages 1934–1941, 2009.

[79] Wilfred F. van Gunsteren and Moritz Winger. Reply to the 'Comment on "On using a too large integration time step in molecular dynamics simulations of coarse-grained molecular models"' by S. J. Marrink, X. Periole, D. Peter Tieleman and Alex H. de Vries, Phys. Chem. Chem. Phys., 2010, 12, DOI: 10.1039/b915293h. *Phys. Chem. Chem. Phys.*, 12:2257–2258, 2010.

[80] S.O. Yesylevskyy, L.V. Schäfer, D. Sengupta, and S.J. Marrink. Polarizable water model for the coarse-grained MARTINI force field. *PLoS computational biology*, 6(6):e1000810, 2010.

[81] Leonardo Darre, Matias R. Machado, Pablo D. Dans, Fernando E. Herrera, and Sergio Pantano. Another Coarse Grain Model for Aqueous Solvation: WAT FOUR? *Journal of Chemical Theory and Computation*, 6(12):3793–3807, 2010.

[82] AJ and Rader. Coarse-grained models: getting more with less. *Current Opinion in Pharmacology*, 10(6):753 – 759, 2010. <ce:title>Endocrine and metabolic diseases/New technologies - the importance of protein dynamics</ce:title>.

[83] S. Riniker and W.F. van Gunsteren. A simple, efficient polarizable coarse-grained water model for molecular dynamics simulations. *The Journal of chemical physics*, 134:084110, 2011.

[84] P. Carbone, H.A.K. Varzaneh, X. Chen, and F. Müller-Plathe. Transferability of coarse-grained force fields: The polymer case. *The Journal of chemical physics*, 128:064904, 2008.

[85] V.A. Harmandaris, D. Reith, N.F.A. van der Vegt, and K. Kremer. Comparison between coarse-graining models for polymer systems: Two mapping schemes for polystyrene. *Macromolecular chemistry and physics*, 208(19/20):2109, 2007.

[86] F. Ercolessi and J.B. Adams. Interatomic potentials from first-principles calculations: the force-matching method. *EPL (Europhysics Letters)*, 26:583, 1994.

[87] S. Izvekov and G.A. Voth. A multiscale coarse-graining method for biomolecular systems. *The Journal of Physical Chemistry B*, 109(7):2469–2473, 2005.

[88] S. Izvekov and G.A. Voth. Multiscale coarse graining of liquid-state systems. *The Journal of chemical physics*, 123:134105, 2005.

[89] A.P. Lyubartsev and A. Laaksonen. Calculation of effective interaction potentials from radial distribution functions: A reverse Monte Carlo approach. *Physical Review E*, 52(4):3730, 1995.

[90] C.D. Berweger, W.F. van Gunsteren, and F. Müller-Plathe. Force field parametrization by weak coupling. Re-engineering SPC water. *Chemical physics letters*, 232(5-6):429–436, 1995.

[91] D. Reith, M. Pütz, and F. Müller-Plathe. Deriving effective mesoscale potentials from atomistic simulations. *Journal of computational chemistry*, 24(13):1624–1636, 2003.

[92] A.J. Rzepiela, M. Louhivuori, C. Peter, and S.J. Marrink. Hybrid simulations: combining atomistic and coarse-grained force fields using virtual sites. *Phys. Chem. Chem. Phys.*, 2011.

[93] S. Jain, S. Garde, and S.K. Kumar. Do inverse Monte Carlo algorithms yield thermodynamically consistent interaction potentials? *Industrial & engineering chemistry research*, 45(16):5614–5618, 2006.